Water and Small Molecule Permeation of Dormant *Bacillus subtilis* Spores

Scott M. Knudsen[1], Nathan Cermak[2], Francisco Feijó Delgado[1], Barbara Setlow[3], Peter Setlow[3]* and Scott R. Manalis[1, 4]*

Departments of [1]Biological and [4]Mechanical Engineering, [2]Program in Computational and Systems Biology, Massachusetts Institute of Technology, Cambridge, MA 02139, and [3]Department of Molecular Biology and Biophysics, UConn Health, Farmington, CT 06030-3305

Running title: *B. subtilis* spore permeability

Keywords: *Bacillus subtilis*, spores, inner membrane, spore permeability, spore outer membrane, spore coat

*Co-corresponding authors

Scott R. Manalis
Address: 77 Massachusetts Ave, 76-261, Cambridge MA 02139
Phone: (617) 253-5039
Email: srm@mit.edu

Peter Setlow
Address: 263 Farmington Ave, Farmington, CT 06030-3305
Phone: (860) 679-2607
Email: setlow@uchc.edu

Abstract

We use a suspended microchannel resonator to characterize the water- and small molecule permeability of *Bacillus subtilis* spores based on spores' buoyant mass in different solutions. Consistent with previous results, we find that the spore coat is not a significant barrier to small molecules, and the extent to which small molecules may enter the spore is size dependent. We have developed a method to directly observe the exchange kinetics of intra-spore water with deuterium oxide, and we apply this method to wild-type spores and a panel of congenic mutants with deficiencies in the assembly or structure of the coat. Compared to wild-type spores that exchange in approximately 1 sec, several coat-mutant spores are found to have relatively high water permeability with exchange times below the ~200 msec temporal resolution of our assay. In addition, we find that the water permeability of the spore correlates with the ability of spores to germinate with dodecylamine and with the ability of $TbCl_3$ to inhibit germination with L-valine. These results suggest that the structure of the coat may be necessary for maintaining low water permeability.

Importance

Spores of *Bacillus* species cause food spoilage and disease, and are extremely resistant to standard decontamination methods. This hardiness is partly due to spores' extremely low permeability to chemicals, including water. We present a method to directly monitor the uptake of molecules into *B. subtilis* spores by weighing spores in fluid. The results demonstrate the exchange of core water with sub-second resolution and show a correlation between water permeability and the rate at which small molecules can initiate or inhibit germination in coat-damaged spores. The ability to directly measure the uptake of molecules in the context of spores with known structural or genetic deficiencies is expected to provide insight into the determinants of spores' extreme resistance.

Introduction

Spores of some *Bacillus* and *Clostridium* species are causative agents of a number of human and animal diseases, as well as food spoilage and food poisoning (1). This is because spores are extremely hardy and can survive mild decontamination procedures that kill growing bacteria. While a number of factors are responsible for spores' high resistance, one factor is their low permeability to many toxic chemicals, in particular chemicals that can damage spore DNA that is located in the central spore core (2-7). There are a number of permeability barriers in the dormant spore. The outermost is the exosporium found on spores of some but not all species, which prevents permeation by very large molecules (> 150 kDa) (8). Moving inward, the second permeability barrier is the spore coat layer plus the underlying outer spore membrane (3, 5). It is not clear that the outer membrane remains intact in dormant spores, although older data suggest that there is a permeability barrier just below the coats (4, 9, 10). This coat/outer membrane barrier restricts access of smaller molecules (> 2-8 kDa) to inner spore regions, in particular the spores' large peptidoglycan cortex just below the outer spore membrane. As a consequence, intact spores and spores with minor coat defects are resistant to peptidoglycan hydrolases such as lysozyme, but spores with severe coat defects are lysozyme sensitive (5, 11).

The final known spore permeability barrier is the inner membrane (IM) surrounding the central spore core. The IM has a lipid composition similar to that in growing/sporulating cells, but lipid probes incorporated into the IM during sporulation are immobile (12, 13). Methylamine, a small molecule that can be accumulated at high levels in spores because of the low core pH, is often used to probe the integrity of the IM because its rate of entry into the spore core is slower than water. Indeed, IM permeability to methylamine is very low, and this low permeability is even retained in spores that lack a coat and outer membrane (2, 14, 15). However,

71 damaging the IM with oxidizing agents can significantly increase its permeability to
72 methylamine (16).

73 The degree to which water is permeable into various compartments of dormant spores is
74 poorly understood. All spore compartments contain water, although the core is thought to be
75 only ~ 30% water by weight while outer spore layers are ~ 80% water (17, 18). Water does
76 penetrate through the entire spore core, and there are several reports that rates of water
77 movement across the IM are rather low, as is movement of other small molecules into the spore
78 core (1, 18-23). However, other reports suggest that the barrier to water entry into the spore core
79 is not exclusively the IM (4, 9, 10, 22). Therefore, the question of whether the IM truly is the
80 barrier to water entering the spore core remains an open one.

81 In order to further examine the permeation of water into dormant *Bacillus subtilis* spores,
82 we have quantified the content of spore material and the extent to which small molecules can
83 permeate the spore based on buoyant mass. Buoyant mass – the weight of a spore in fluid
84 (Equation 1) – is determined by weighing single spores as they pass through, or are trapped
85 within a suspended microchannel resonator (SMR). We have also developed a method to track
86 spores' buoyant mass as their internal H_2O is replaced with heavy water (D_2O), and have
87 analyzed this water movement in spores of a number of congenic mutant *B. subtilis* strains with
88 defects in the coat/outer membrane of varying severity. Finally, we tested for the permeation of
89 the outer layers of these spores to Tb^{3+} ions and dodecylamine using a germination assay.
90 Interestingly, we found that water permeation measured by the SMR could be used to predict the
91 permeation of Tb^{3+} ions and dodecylamine. Overall, the findings in this work provide new
92 information on the permeation of water and other small molecules into various compartments of

93 a dormant spore and demonstrate that the structure of the coat is important for maintaining low
94 water permeability.

Materials and Methods

***B. subtilis* strains used and spore purification.** The wild-type *B. subtilis* strain used in this work was strain PS533 (24), a derivative of strain PS832, a prototrophic laboratory 168 strain; strain PS533 carries plasmid pUB110 providing resistance to kanamycin (10 μg/ml). All other strains are listed in Table 1, and are congenic with strain PS533, but lack plasmid pUB110. Strain PS4427 was constructed by transforming strain PS3738 (*safA*) to chloramphenicol resistance with DNA from strain PS3740 (*cotE*).

Spores of all strains were prepared at 37°C on 2x Schaeffer's-glucose medium agar plates (25, 26) without antibiotics. Plates were incubated for 2-3 d at 37°C, and then for 2-4 d at 23°C to allow extensive autolysis of sporulating cells and cell debris. The spores were then scraped from plates into cold deionized water, and spores were purified at 4°C over ~ 7 d by multiple rounds of centrifugation, washing pellets with cold water to remove debris, and with brief sonication between centrifugation to further disrupt debris. Purified spores were stored at 4°C in water protected from light. All spores used in this work were > 98% free of growing or sporulating cells, germinated spores and cell debris as determined by phase contrast microscopy.

Spore germination. Spores of various strains were germinated with either L-valine or dodecylamine essentially as described (27, 28). In all cases, spore germination was monitored by measuring the release of the spore core's large depot (~20% of core dry wt) of dipicolinic acid (DPA) by its fluorescence with Tb^{3+} either by inclusion of $TbCl_3$ in germination solutions, or by removal of 180 μl aliquots of germination mixes incubated without $TbCl_3$ and addition of 20 μl of 500 μM $TbCl_3$. Specific germination conditions were as follows. For L-valine germination, spores at an optical density at 600 nm (OD_{600}) of 2.0 were first heat activated for 30 min at 75°C, and then cooled on ice for at least 10 min. Spores at an OD_{600} of 0.5 were germinated at 37°C in

200 µl of 25 mM K-Hepes buffer (pH 7.4) – 50 µM $TbCl_3$ – 10 mM L-valine, which is a saturating concentration for this germinant. These mixtures were incubated in a multi-well fluorescence plate reader, and Tb-DPA fluorescence was read every 5 min. For analysis of L-valine germination without Tb present throughout germination, 2-3 ml germination mixtures with the same conditions described above, but without $TbCl_3$, were incubated in a water bath at 37°C; at various times 180 µl aliquots were added to 20 µl of 500 µM $TbCl_3$, and the fluorescence of the mixture was read immediately as described above.

Dodecylamine germination of spores is not stimulated by heat-activation (27) and was carried out in the absence of $TbCl_3$ as described above for L-valine germination, but with 0.8 mM dodecylamine and at 50°C. Again, 180 µl aliquots of germination mixtures were added to 20 µl of 500 µM $TbCl_3$ and the fluorescence was read as described above. The amount of total DPA in all spores used for germination experiments was determined by boiling spores for 30 min, centrifuging and measuring DPA in the supernatant fluid by its fluorescence with Tb^{3+} as described previously (28, 29). These total DPA values were used to determine percentages of spore germination in all germination experiments.

Buoyant mass determination in a Suspended Microchannel Resonator (SMR). The SMR is a microfluidic device that consists of a fluid channel embedded in a vacuum-packaged cantilever (30). The cantilever resonates at a frequency proportional to its total mass, and as an individual spore travels through the embedded microchannel, the total cantilever mass changes. This change in mass is detected as a change in resonance frequency that corresponds directly to the buoyant mass of the spore. Buoyant mass is the weight of the spore in fluid and is equivalent to the mass of the spore in excess of the fluid that it displaces, as shown in Equation 1 where m, V, and ρ are the mass, volume, and density of the spore and ρ_{fluid} is the density of the solution.

$$m_b = V(\rho - \rho_{fluid}) = m\left(1 - \frac{\rho_{fluid}}{\rho}\right) \qquad \text{Eq. (1)}$$

We used a 120 μm long SMR with an internal fluid channel of 3 μm x 5 μm, driven in the second vibrational mode (f ~2.1 MHz). A schematic of the cantilever with embedded fluid channel is shown in Fig 1a. The chip containing the SMR is mounted on a fluidic manifold and computer controlled pressure regulators with pressurized glass sample vials are used to precisely control fluid flow within the SMR as previously described (31). Spores are suspended in the desired solution, allowed to equilibrate for 30 min, and loaded into the sample bypass channel. Sample fluid is directed through the resonator and the buoyant mass for individual spores is determined as they flow through the cantilever.

Centrifugal trapping and spore water exchange. Bacterial spores can be 'trapped' at the end of the cantilever when centrifugal force (proportional to the vibrational amplitude squared) becomes greater than the force due to fluid flow through the channel (32). To initiate trapping of bacterial spores, the drive amplitude is increased until spores are efficiently trapped at the tip of the resonator at the desired flow rate. Spores are suspended in a solution of sucrose in H_2O at ~25% w/v (adjusted to match the density of D_2O, ~1.1 g/mL) and are loaded into one bypass channel of the SMR chip. The other bypass channel is loaded with pure D_2O. The direction of flow through the resonator is reversed, replacing the sample solution from the first bypass channel with D_2O from the second. A schematic representation of spore trapping and fluid exchange is shown in Fig1a-c. As indicated in the results section, some experiments are performed with the exchange between solutions in the reverse of this order. The background signal that results from fluid exchange in an empty resonator is recorded prior to trapping any spores. Spores enter the cantilever and are trapped at the tip, where they remain during subsequent exchange from the sample solution to D_2O. Spores are exchanged back into the

sample solution, from which additional spores enter the trap. Multiple rounds of exchange with successive trapping of spores are performed. The resonator frequency is recorded throughout these exchanges and the signal due to the buoyant mass of the spores is obtained by subtracting the background signal. The change in buoyant mass is calculated from the difference in baseline frequencies between the two solutions before and after the trapping of spores (Fig 1d).

Results

Buoyant mass. Buoyant mass quantifies how much a spore weighs in excess of the fluid that it displaces (see Materials and Methods). The buoyant mass of a spore in solutions of two different densities can be used to calculate the mass, volume, and density of the cell. Likewise, measurements in H_2O and D_2O solutions can be used to separately quantify the dry and aqueous contents (31). To determine the distribution across the population, the buoyant mass of ~1000 individual hydrated *B. subtilis* (PS533; wild-type) spores is determined by weighing them in an SMR. Buoyant mass profiles for spores determined in H_2O ($\rho \sim 1.0$), in 97.5% D_2O ($\rho \sim 1.1$ g/mL), and in H_2O solutions of glycerol, sucrose, and Percoll (colloidal suspension) at ~ 1.1 g/mL are shown in Fig. 2a. Spores in H_2O have a density of ~1.2 g/cm^3 determined by density gradient ultracentrifugation (33) and therefore have a positive buoyant mass because they weigh more than the H_2O that they displace. For these measurements, spores have the greatest buoyant mass in water. The other fluids are all prepared at the same density (1.1 g/mL) and result in a reduced buoyant mass relative to measurements in pure H_2O because the difference between spore density and solution density is lower. The buoyant masses of solid particles in the four solutions at 1.1 g/mL are equivalent because the particles displace an equal volume (and mass) of each fluid (data not shown). However, spores are not solid particles, and the molecules in each solution can permeate the spore to different extents, as shown schematically in Fig. 2b. Molecules that have permeated into the spore add to the buoyant mass determined for each spore as they displace less dense H_2O molecules.

Physical properties of intact spores. The size and density of a spore determines its buoyant mass in a given solution. Because these parameters vary from spore to spore, we obtain a distribution of buoyant masses under each condition (Fig 2a). Several biophysical parameters for

192 the wild-type spore population can be calculated from the buoyant mass distributions shown in
193 Fig 2a. For example, the median buoyant mass of the spores in H_2O (165 fg; coefficient of
194 variation [CV] 23%) and Percoll (89 fg; CV 36%) define a line for which the slope is an estimate
195 of the median spore volume (0.76 μm^3). The x-intercept is an estimate of the spore density
196 (assuming all spores are equally dense), which we calculate as 1.22 g/cm^3, a value nearly
197 identical to that determined by ultracentrifugation on a Percoll gradient (33). Although the
198 population data collected here cannot directly address variability in single spore volume and
199 density, if we assume all spores are equally dense, then the volume CV is equal to the buoyant
200 mass CV. The assumption of roughly constant density is likely valid, given previous work
201 showing variation in cell size is generally far greater than in cell density (34-36). Indeed, dry
202 spore volumes quantified by electron microscopy (35) show a CV of 21%, similar to what we
203 observe for buoyant mass.

204 As with the measurements in water and in Percoll, we can also compare differences
205 between buoyant mass measurements in H_2O and D_2O to estimate properties of the dry spore.
206 Because D_2O molecules entirely replace H_2O throughout the spore, only the dry content is
207 responsible for the difference in buoyant mass between these solutions. The line between the
208 buoyant masses in H_2O and D_2O (128 fg; CV 18%) determines the dry volume to be 0.37 μm^3
209 and the dry density to be 1.45 g/cm^3, which is also consistent with previously determined values
210 (33).

211 The H_2O content of spores can be calculated based on the difference between the total
212 spore content and the dry spore content. If we extrapolate the lines shown in Fig. 2c back to a
213 solution density of 0 g/mL, the y-intercepts (not shown) would represent the median spore's total
214 mass and dry mass. The difference between the two is the mass of the spores' H_2O, estimated

here to be 390 fg. Alternately, any two points of equivalent density on these lines can be subtracted to find the buoyant mass of the H_2O with respect to the solution density. As shown in Fig. 2c, a spore is 39 fg heavier in D_2O than in Percoll. H_2O is only 0.1 g/mL less dense than D_2O (1.1 g/mL), so to obtain the total H_2O content (density of 1.0 g/mL) the difference between the Percoll and D_2O measurements must be scaled by a factor of ten.

Molecular permeation based on buoyant mass. The above determination of H_2O content represents the extremes of spore permeability. Percoll is a colloidal suspension of 15-30 nm polyvinylpyrrolidone-coated silica particles that are expected to be completely excluded from spores, whereas D_2O is not excluded at all and can entirely replace a spore's internal H_2O. In between these extremes, small molecules can permeate some portion of solvent space within the spore. The cortex of a spore is accessible to small molecules, such as nutrients that must reach the IM to initiate germination, although it is traditionally difficult to measure the volumes accessible to these molecules. By measuring the buoyant mass of spores in solutions of small molecules of various sizes, we show that it is possible to probe the internal volume of the spore that is accessible to these molecules (Fig. 2b). We have chosen neutral, highly soluble molecules for this assay to minimize the extent to which they interact with the spore. However we note that chemical interactions or other forces which concentrate molecules within the spore will increase the buoyant mass of the spores. Similarly, repulsion or exclusion of these molecules would decrease the buoyant mass of spores. The median buoyant mass of wild-type spores in the sucrose and glycerol solutions is 111 fg (CV 19%) and 117 fg (CV 21%), respectively. When compared to the Percoll measurement, we observe that an additional buoyant mass of 22 fg sucrose and 28 fg glycerol can permeate the outer layers of the spore at these concentrations. Assuming a uniform distribution of these molecules, the additional mass in glycerol relative to

238 sucrose indicates that there is a greater volume within the cortex that is accessible to glycerol,
239 and this is consistent with previous work on the levels to which different molecules can permeate
240 the spore (4). If we assume that these solutes diffuse into the spore's interior volume to the same
241 concentration as that outside the spore, these values suggest that of the 0.39 μm^3 occupied by
242 water, 0.22 μm^3 is accessible to sucrose and 0.28 μm^3 is accessible to glycerol.

243 **Physical properties and permeation in coat-defective spores.** Due to the fact that they lack
244 most coat layers (37), spores with mutations in both *cotE* and *gerE* genes have been
245 characterized in the literature by a number of different techniques. Relevant to the studies herein,
246 the near-total lack of a coat has been directly visualized by atomic force microscopy (AFM) (38),
247 and they have been found to have significantly more rapid core water permeability than wild-
248 type (22). The buoyant masses of *cotE gerE* spores were determined for the same solutions
249 described above (Fig 2d). Overall, the buoyant masses for these spores are lower than wild-type
250 spores. Because a number of the genes regulated by GerE are not specific to the assembly of the
251 coat (39), it is likely that some of the mass difference is due to loss of specific proteins or
252 structures besides just the coat. Nevertheless, the loss of coat biomaterial (and hence buoyant
253 mass) is consistent with observations from AFM that these spores are almost entirely devoid of a
254 coat (38). Therein, it was noted that some spores still retain patches of coat material. We note
255 that there appear to be two peaks in the buoyant mass distribution for *cotE gerE* spores. For
256 example, in the blue line in Fig 2d, where the spores' buoyant masses were determined in H_2O,
257 the population has a median buoyant mass of 95 fg (CV 26%), however the left hand portion of
258 this distribution appears to be a primary population with a lower buoyant mass centered at ~90
259 fg, and a less abundant sub-population centered at ~130 fg, which we suspect are spores that
260 retain a portion of their coat.

The permeability to molecules in *cotE gerE* spores is also very different from wild-type spores. The median buoyant masses of these spores in glycerol and sucrose are identical (67 fg; CV 27%), suggesting that both of these molecules enter the spore to the same extent. Unlike intact spores, spores with severely damaged coats cannot exclude larger molecules from the peptidoglycan cortex, hence many coat mutants become lysozyme sensitive (11). The median buoyant mass is 65 fg (CV 23%) in Percoll, which consists of colloidal silica particles that are large relative to glycerol and sucrose molecules. The fact that sucrose and glycerol increase the buoyant mass to the same degree as each other and only slightly more than Percoll suggests that the cortex is not providing a differential barrier to these different-sized molecules in *cotE gerE* spores as it does in wild-type spores. This suggests that the cortex of coat-damaged spores has open volumes that are much more accessible to external solvent than in intact spores. As noted above, some changes in cortex structure may exist in this mutant beyond those caused by the lack of a coat, due to the variety of genes regulated by GerE (39). Interestingly, the shape of the buoyant mass distribution for these spores is different in Percoll than in other solutions, and the heavier subpopulation is no longer apparent. If this population were to exclude Percoll from some interior volume, the space would remain filled with only H_2O, and the spore would weigh less than if the volume were filled with a heavier solution.

To calculate the H_2O content of *cotE gerE* spores, we subtract the median buoyant mass in Percoll (65 fg; CV 23%) from that in D_2O (76 fg; CV 26%), yielding a H_2O buoyant mass of 11 fg. Note that 11 fg buoyant mass from H_2O when weighed in a solution density of 1.1 g/mL is equivalent to 110 fg total H_2O mass. Glycerol (the smallest of the permeating molecules) is expected to approach the IM to a similar extent as H_2O. If this is true, the 9 fg buoyant mass of H_2O (90 fg total mass) that glycerol cannot replace represents mostly core H_2O.

Kinetics of buoyant mass change. The buoyant mass measurements for Fig. 2 are useful for measuring the characteristics of a population at equilibrium or undergoing slow changes (on the order of minutes or more), but water permeation of spores occurs on a timescale of seconds or less. To study spore water permeation on a sub-second timescale, we developed a technique to trap spores at the tip of the cantilever and monitor the spore's buoyant mass during the transition between two fluids, as shown schematically in Fig. 1. For a typical assay, spores are initially suspended in a sucrose solution at ~1.1 g/mL and are exchanged into pure D_2O. The change in buoyant mass that occurs for PS533 (wild-type) spores is shown in Fig. 3a. Data are aligned such that t=0 is the time when the fluid exchange in an empty resonator is complete. Curves of increasing magnitude are the result of successively trapping multiple spores, annotated to the right of the curves, and repeating the fluid exchange. The y-axis for these plots represents the change in buoyant mass of the spores between the two solutions, and is determined from the difference between the mass signals – SMR resonant frequency – in each fluid, as shown in Fig 1d,e.

Exchanging spores from a sucrose/H_2O solution to D_2O results in the movement of all three of these species within different parts of the spore. In Fig. 3a, we observe an increase in mass consistent with the replacement of H_2O with D_2O. We also expect the sucrose molecules from the initial solution to diffuse out of the spores, but we do not observe a loss in mass over the several sec following the fluidic exchanges. This suggests that either the sucrose leaves the spores concurrently with (or more quickly than) replacement by D_2O, or the sucrose leaves over a timescale that is longer than a few sec, illustrated schematically in Fig. 3b. The buoyant mass obtained from the spore populations (Fig. 2) can be used to inform our interpretation of the kinetic data. Population data are acquired over a much longer time period (30-60 min) and can be

307 considered as end points for the exchange kinetics. According to the median population values
308 reported above, we expect each spore to gain ~39 fg buoyant mass due to uptake of D_2O, and to
309 lose ~ 22 fg buoyant mass of sucrose; a net increase of ~17 fg.

310 To determine if the kinetic measurements are consistent with the end-point population
311 measurements, we repeatedly measured the buoyant mass of spores ~9 sec after a fluid switch
312 from sucrose in H_2O to D_2O and normalized to the number of spores that were trapped in the
313 resonator at the time (Fig. 3c). To account for experimental variation outside of calculated error
314 bars (Supplemental Material), values and standard errors reported here are determined from
315 replicate fluid switches in which at least 10 spores were trapped in the resonator. The per-spore
316 mass change after ~9 sec in D_2O is 17.9 ± 0.6 fg, (mean ± SE). Similarly, an exchange in which
317 the spores were switched into D_2O for 1 min prior to the buoyant mass determination (green dots
318 in Fig. 3c) yields a value of 17.7 ± 0.8 fg. The close agreement between these values and the
319 estimate of the population endpoint (17 fg) shows that the bulk of the sucrose leaves the spore
320 either faster than or concurrent with the exchange of H_2O for D_2O. However, a careful error
321 analysis reveals that it is still possible for a buoyant mass of up to 1.7 fg of sucrose to remain
322 within the spore and not be detected by our method (Supplemental Material).

323 **Water permeability of coat-mutant spores.** Previous analysis by NMR has shown that *cotE*
324 *gerE* mutant spores have a greatly increased water permeability (20). Fig 3d shows the result of
325 our fluid exchange analysis on these spores. Unlike the wild-type spores shown in Fig. 3a, fluid
326 exchange with *cotE gerE* spores appears to already be complete by the time the resonator is fully
327 flushed (~200 msec) (Fig. 3d), which is consistent with the previous report using NMR. CotE is
328 a protein required for normal coat assembly, and *cotE* spores lack a number of coat proteins and
329 appear to lack an outer coat (5). GerE is a transcription factor that regulates a number of proteins,

330 many of which are involved in assembly of the coat, but also many others which control
331 disparate processes during spore formation (39). Thus, while these spores are severely coat
332 defective, there may be other aspects of this mutant that affect its water permeability.

333 In order to address the importance of the coat to spore water permeability, we have
334 characterized water exchange for spores with a number of additional mutations that are known to
335 affect coat formation (Fig. 4). Kinetic traces for mutants not shown above (Fig 3) are presented
336 in Supplemental Material Fig S2, and time constants determined for all spores are shown in Fig
337 4. The time constants determined for these exchange reactions suggest that all coat mutations
338 studied here affect the permeability of the resulting spore at some level. On the extreme end,
339 several coat mutations appear to completely abrogate the relatively slow exchange seen with the
340 wild-type spores. The *gerE* and *safA* mutations (alone or in conjunction with *cotE*) result in
341 spores whose H_2O appears to have been nearly completely exchanged within the time required to
342 fully flush the cantilever with D_2O, as does the *spoVID* mutation. We estimate 0.09 sec as an
343 upper bound on the time constant for these spores.

344 The *cotE* mutation results in spores for which most of the H_2O has exchanged by t=0,
345 although there is some observable exchange. It is interesting to note that significant
346 heterogeneity in coat structure has been observed by AFM of *cotE* spores (38). It may be that this
347 mutation results in spores with differential permeability to water as well, with less permeable
348 spores contributing to the amplitude of the observed exchange and quickly-exchanging spores
349 only contributing to the overall amplitude of the curves. Indeed, for *cotE* spores, 80% of the H_2O
350 is exchanged within the time required to flush the channel, while for the *cotH* and *cotXYZ*
351 mutants, whose exchange rates are equivalent to *cotE*, this value is ~50% (Fig S2). The H_2O
352 exchange for *cotO* and *cotB* spores is increasingly slow, suggesting these mutations have a less

353 deleterious effect on spore water permeability. Interestingly, a *cotXYZ* mutant that results in the
354 loss of spores' outermost crust layer also resulted in increasing spore water permeability similar
355 to that of *cotH* spores (Fig. 4).

356 **Molecular permeation based on spore germination.** The results described above indicated that
357 coat defects have significant effects on permeation of molecules including water into spores. To
358 examine if this is also the case for other small molecules that are thought to exert their effects by
359 acting at a spore's inner membrane just outside of the spores core, we examined spores'
360 permeation by two compounds, Tb^{3+} and dodecylamine, that can influence spores' return to life
361 in the process of germination (27, 29, 34). $TbCl_3$ at ~ 50 μM is often used to monitor the
362 progress of spore germination, by measuring DPA release via Tb-DPA complex formation (28).
363 $TbCl_3$ at 50 μM only minimally inhibits the germination of intact spores, but completely inhibits
364 the germination of severely coat defective spores (29). The mechanism for this inhibition has not
365 been definitively established, but it has been suggested that Tb^{3+} binds to DPA being released
366 from the protein channel in spores' IM through which DPA is released and the Tb-DPA complex
367 blocks this channel completely. If this is the case, then Tb^{3+} would need to penetrate to the IM to
368 inhibit spore germination, something that should be much easier in coat-defective spores. To test
369 the effects of $TbCl_3$ on the germination of the wild-type and various coat mutant *B. subtilis*
370 spores used to measure water permeation, we monitored the germination of these spores with the
371 nutrient germinant L-valine with Tb^{3+} either present throughout the germination process or only
372 added at various times (Fig. 5a,c,e; and data not shown). Notably spores of all severely coat
373 defective strains (i.e. those which produce lysozyme sensitive spores (11); *safA, spoVID, cotE*,
374 *gerE*, *cotE gerE,* and *cotE safA*) exhibited complete or almost complete lack of germination in
375 the continuous presence of $TbCl_3$, although these spores germinated reasonably well in the

absence of Tb^{3+}. The *cotH* and *cotXYZ* spores exhibited less significant inhibition of spore germination by $TbCl_3$, with spores of other coat-defective strains exhibiting only minimal inhibition (Fig. 4, 5). The sensitivity of spore mutants to inhibition of germination by Tb^{3+} appears to be correlated with the water permeability of the core (Fig 4).

While spores normally germinate with nutrient germinants such as L-valine, they also germinate with some non-nutrient germinants, such as cationic surfactants like dodecylamine (27). This molecule most likely triggers germination by directly opening spores' IM channel for DPA, probably by binding to SpoVAC, one of the seven IM SpoVA proteins that likely comprise this channel (27, 40, 41). In order to bind to SpoVAC, the dodecylamine must penetrate through spores' outer layers to access the IM, and it is certainly possible that rates of spore germination with dodecylamine could be dependent on the rate of permeation of this agent through spores' outer layers. Indeed, chemical decoating and at least one severe coat defect increase rates of dodecylamine germination of *B. subtilis* spore germination markedly (27). Examination of the rates of dodecylamine germination of the wild-type and coat mutant spores with $TbCl_3$ added at various times in germination gave results that were concordant with those seen with effects of $TbCl_3$ on L-valine germination (Fig. 5b,d,f; and data not shown). Thus the more severely coat defective spores (*safA, spoVID, cotE*, *gerE*, *cotE gerE,* and *cotE safA*) and had much higher rates of dodecylamine germination than wild-type, *cotO*, *cotB*, *cotH,* or *cotXYZ* spores. The germination of mutant spores with dodecylamine also appears to correlate with the water permeability of the spore core (Fig 4).

Discussion

We report here a method for observing the water- and small molecule permeability of bacterial spores based on the buoyant mass of these particles in different solutions and on the increase in mass that occurs when internal H_2O is replaced by D_2O. While it was once hypothesized that water in the core of *B. subtilis* spores was essentially immobile, it has been demonstrated that spore core water is: i) mobile; and ii) free to exchange with external water, albeit at a rate which is significantly slower than that for vegetative cells (4, 17, 20, 22). It has generally been regarded that permeability of the inner membrane that surrounds the core is the primary barrier to exchange with external water.

The IM of coat-defective spores has permeability to methylamine and lipid mobility similar to that of wild-type (12-15). However, we find that the rate at which core water is exchanged is altered significantly for a number of coat mutants, with several mutations that exchange faster than the ~200 msec temporal resolution of our assay. Similarly, measurements of water ^2H relaxation rates by NMR spectroscopy indicate that the water permeability of the *B. subtilis* spore IM is ~25-fold greater in *cotE gerE* spores than in wild-type spores (22), and decoating spores also increases rates of ^{129}Xe movement into the spore core (21). Two possible explanations for this apparent discrepancy are: i) the IM is the barrier to exchange of core water in wild-type spores, but that barrier becomes defective in damaged spores. If this is the case, then the permeability of the IM may require the integrity of spores' outer layers, which affect IM structure in a way that alters its permeability to water but not to methylamine. ii) The IM is not the barrier to water entering the spore core, in which case some structure outside the IM must provide this barrier.

418 Here we investigate the role of the spore coat in maintaining the low water permeability
419 of the core. We find that spores lacking CotB, a major component of the outer coat, have
420 permeability similar to that of wild-type. Spores lacking CotO or CotH, which control the
421 assembly of a number of outer coat proteins display more significant increases in the rate of
422 water exchange. Similarly loss of CotE, which localizes to a layer between the inner and outer
423 coat and guides outer coat formation, results in even faster exchange. Although this trend
424 suggests that proteins residing between the outside of the spore and the inner coat have
425 increasing effects on the rate of water exchange, *cotXYZ* spores, which lack the outermost crust
426 layer, display an exchange rate equivalent to that of *cotE* spores. Consistent with this result, it
427 has been suggested that the spore crust may contribute to the structure of the outer coat, as this
428 layer is easily disrupted in spores lacking CotXYZ (42). All of the other mutations tested
429 exchange water faster than the current limit of detection of this assay. Of these, SpoVID and
430 SafA are both involved early in coat formation and GerE is a transcription factor that regulates
431 many proteins involved in coat formation, as well as other processes (39). Double coat mutant
432 spores, which have increased loss of coat material also exchange faster than the limit of this
433 assay.

434 The coat itself likely cannot be a barrier to water, as it does not provide a barrier to
435 molecules that are much larger. For instance, it has long been known that small molecules can
436 permeate the coat and beyond (4) and dyes used to determine the surface area of spores confirm
437 this porous nature (43). However, we find that removing or compromising the coat removes the
438 barrier to core-water permeability. One possibility is that upon exiting the core, water interacts
439 specifically with outer layers of the spore in a way that small molecules cannot. The cortex of the
440 spore is hygroscopic, and mechanical changes occurring on the same timescale as those observed

441 herein have been observed for spores upon changes in relative humidity (44). However these
442 changes still occur in *cotE gerE* spores, whereas these mutations abolish the low water
443 permeability in this work and as observed by NMR. If the mechanism connecting these disparate
444 spore regions involves the intermediate layers, in particular the cortex, either by the creation of
445 an alternate barrier or by modulation of an existing barrier (the IM), measuring the molecular and
446 water permeability of spore cortex- or other mutants could provide additional insights. For
447 example, we may find mutations that change the structure of the cortex or of the inner membrane
448 in a way that abolishes this barrier even in the presence of an intact coat.

449 The data presented here also show a correlation between the rate at which spores
450 exchange H_2O with external D_2O and the ability of both Tb^{+3} and dodecylamine to gain access to
451 the IM, as measured by a germination assay. In addition, wild-type spores are shown to allow a
452 greater extent of permeation to small molecules than to larger ones, a characteristic that is
453 abolished in coat-defective spores. Taken together, these results support the notion that
454 molecular access to the IM (the rate at which molecules are able to get up to the IM) may limit
455 the rate at which molecules are able to cross the IM, even for molecules as small as water.

456 The space that appears to be freely solvent accessible within a *B. subtilis* spore is in the
457 coat and the peptidoglycan cortex (4, 17, 45). In a simple biophysical model of the spore, we
458 might envision the cortex as a series of water- and small molecule-accessible spaces of
459 decreasing size as one approaches the core. We would expect that the larger, outer accessible
460 areas are essentially open space relative to the size of molecules, but at some point become
461 restrictive on this scale. That is, solvent-accessible space within the cortex may simply keep
462 decreasing as one approaches the core to the extent that there are simply very few places through
463 which water and other molecules can pass to access the inner membrane. This model is

consistent with our observation that glycerol (92.1 Da) can invade the spore to a greater extent than sucrose (342.2 Da), as was also observed by bulk solute uptake measurements for molecules differing by four orders of magnitude in molecular weight (4).

The bulk of cortex space is indeed freely accessible, as we find that the majority of the sucrose leaves the spore on a timescale this is either comparable or faster than the H_2O/D_2O exchange. Under the model proposed above, we might expect that some small molecules that have been taken up by the spore into areas that are restrictive to their permeation could be observed leaving the spore at a slower rate during the fluid exchange assays. However, while some sucrose may remain in the spore after exchange of water, its loss was not directly observed. Finally a mechanism to form a gradient of solvent-accessible space is not known. This could possibly be achieved by changes in molecular packing or in changes in the structure of the cortex itself. It has been observed that cortex cross-linking appears to be highest at the outer part of the cortex, with 2- to 8-fold lower crosslinking just outside of the germ cell wall adjacent to the IM (46, 47), although it is not clear how crosslinking would affect solvent-accessible space. Subsequent work may elucidate characteristics of the spore that affect their permeability to water and small molecules. Molecular exclusion within the cortex has been demonstrated across a wide range of molecule sizes for *Bacillus cereus* (4), and we show here that while similar permeability differences exist for *B. subtilis* wild-type spores, this difference is abolished in severely coat defective spores. It will be interesting to determine the extent to which these permeability differences exist in spores with only minor coat defects, and if so, whether they show any correlation with the observed loss of a barrier to water permeability.

The SMR provides a direct way to track the motion of molecules into and out of the spore based on the addition or loss of mass, and the use of D_2O enables us to look at the motion of H_2O

487 in addition to dissolved molecules. Similarly, nuclear magnetic resonance (NMR) experiments
488 and Raman spectroscopy have also used D_2O to investigate spore water. The main benchmarks
489 by which we can compare these are the sample size and time scale of the experiments. Raman
490 spectroscopy also has been used to investigate individual spores; however, the temporal
491 resolution of this technique is currently limited to ~2 data points per second (20). NMR
492 experiments can be performed across a wider range of time scales, but are typically made on
493 bulk samples consisting of grams of spores, with additional purity considerations like the need to
494 eliminate manganese ions from spore preparations.

495 The SMR is a microfluidic device capable of using very small sample volumes. For
496 population measurements we typically assay ~1000 individual spores, and kinetic data is
497 available down to the individual spore level, although we typically acquire these data with up to
498 ~20-30 spores. The temporal resolution of our kinetic measurements is ~10 ms and is limited by
499 the stability of the resonator system (Fig S1). For our population measurements, the temporal
500 resolution is limited by the time required to measure a statistically representative number of
501 spores (typically less than an hour). Population measurements may ultimately prove useful for
502 enabling transport properties to be measured over long time scales (hours to days).

Acknowledgements

This work was supported by a Department of Defense Multi-disciplinary University Research Initiative through the U.S. Army Research Laboratory and the U.S. Army Research Office under contract number W911F-09-1-0286 (PS), and by the Institute for Collaborative Biotechnologies through grant W911NF-09-0001 (SRM) from the US Army Research Office. The content of the information does not necessarily reflect the position or the policy of the Government, and no official endorsement should be inferred. We are grateful to Stephanie Luu and Jose Cruz Mora for assistance with spore preparation.

References

1. **Setlow P, Johnson EA.** 2013. Spores and their significance, p. 45-79. *In* Doyle MP, Buchanan R (ed.), Food microbiology, fundamentals and frontiers, 4th ed. ASM Press, Washington, DC.

2. **Cortezzo DE, Setlow P.** 2005. Analysis of factors that influence the sensitivity of spores of *Bacillus subtilis* to DNA damaging chemicals. J Appl Microbiol **98:**606-617.

3. **Driks A.** 1999. *Bacillus subtilis* spore coat. Microbiol Mol Biol Rev **63:**1-20.

4. **Gerhardt P, Black SH.** 1961. Permeability of bacterial spores. II. Molecular variables affecting solute permeation. J Bacteriol **82:**750-760.

5. **Henriques AO, Moran CP.** 2007. Structure, assembly, and function of the spore surface layers. Annu Rev Microbiol **61:**555-588.

6. **Setlow P.** 2006. Spores of *Bacillus subtilis*: their resistance to and killing by radiation, heat and chemicals. J Appl Microbiol **101:**514-525.

7. **Setlow P.** 2013. Resistance of bacterial spores to chemical agents, p.121-130. *In* Fraise AP, Maillard J-Y, Sattar SA (ed.), Principles and practice of disinfection, preservation and sterilization, 5th ed. Wiley-Blackwell, Oxford, UK.

8. **Gerhardt P.** 1967. Cytology of *Bacillus anthracis*. Fed Proc **26:**1504-1517.

9. **Koshikawa T, Beaman TC, Pankratz HS, Nakashio S, Corner TR, Gerhardt P.** 1984. Resistance, germination, and permeability correlates of *Bacillus megaterium* spores successively divested of integument layers. J Bacteriol **159:**624-632.

10. **Rode LJ, Lewis CW, Foster JW.** 1962. Electron microscopy of spores of *Bacillus megaterium* with special reference to the effects of fixation and thin sectioning. J Cell Biol **13:**423-435.

11. **Klobutcher LA, Ragkousi K, Setlow P.** 2006. The *Bacillus subtilis* spore coat provides "eat resistance" during phagocytic predation by the protozoan *Tetrahymena thermophila*. Proc Natl Acad Sci U S A **103:**165-170.

12. **Cowan AE, Olivastro EM, Koppel DE, Loshon CA, Setlow B, Setlow P.** 2004. Lipids in the inner membrane of dormant spores of *Bacillus* species are largely immobile. Proc Natl Acad Sci U S A **101:**7733-7738.

13. **Griffiths KK, Setlow P.** 2009. Effects of modification of membrane lipid composition on *Bacillus subtili*s sporulation and spore properties. J Appl Microbiol **106:**2064-2078.

14. **Setlow B, Setlow P.** 1980. Measurements of the pH within dormant and germinated bacterial spores. Proc Natl Acad Sci U S A **77:**2474-2476.

15. **Swerdlow BM, Setlow B, Setlow P.** 1981. Levels of H^+ and other monovalent cations in dormant and germinating spores of *Bacillus megaterium*. J Bacteriol **148:**20-29.

16. **Cortezzo DE, Koziol-Dube K, Setlow B, Setlow P.** 2004. Treatment with oxidizing agents damages the inner membrane of spores of *Bacillus subtilis* and sensitizes spores to subsequent stress. J Appl Microbiol **97:**838-852.

17. **Gerhardt P, Marquis RE.** 1989. Spore thermoresistance mechanisms, p. 43-63. In Smith I, Slepecky RA, Setlow P (ed.), Regulation of procaryotic development: structural and functional fnalysis of bacterial sporulation and germination. American Society for Microbiology, Washington, DC.

18. **Kaieda S, Setlow B, Setlow P, Halle B.** 2013. Mobility of core water in *Bacillus subtilis* spores by ^2H NMR. Biophys J **105:**2016-2023.

19. **Ghosal S, Leighton TJ, Wheeler KE, Hutcheon ID, Weber PK.** 2010. Spatially resolved characterization of water and ion incorporation in *Bacillus* spores. Appl Environ Microbiol **76:**3275-3282.

20. **Kong L, Setlow P, Li YQ.** 2013. Direct analysis of water content and movement in single dormant bacterial spores using confocal Raman microspectroscopy and Raman imaging. Anal Chem **85:**7094-7101.

21. **Liu G, Bettegowda C, Qiao Y, Staedtke V, Chan KW, Bai R, Li Y, Riggins GJ, Kinzler KW, Bulte JW, McMahon MT, Gilad AA, Vogelstein B, Zhou S, van Zijl PC.** 2013. Noninvasive imaging of infection after treatment with tumor-homing bacteria using Chemical Exchange Saturation Transfer (CEST) MRI. Magn Reson Med **70:**1690-1698.

22. **Sunde EP, Setlow P, Hederstedt L, Halle B.** 2009. The physical state of water in bacterial spores. Proc Natl Acad Sci U S A **106:**19334-19339.

23. **Westphal AJ, Price PB, Leighton TJ, Wheeler KE.** 2003. Kinetics of size changes of individual *Bacillus thuringiensis* spores in response to changes in relative humidity. Proc Natl Acad Sci U S A **100:**3461-3466.

24. **Setlow B, Setlow P.** 1996. Role of DNA repair in *Bacillus subtilis* spore resistance. J Bacteriol **178:**3486-3495.

25. **Nicholson W, Setlow P.** 1990 Sporulation, germination and outgrowth, p 391-450. *In* Harwood C, Cutting S (ed), Molecular biological methods for *Bacillus*. John Wiley and Sons, Chichester, UK.

26. **Paidhungat M, Setlow B, Driks A, Setlow P.** 2000. Characterization of spores of *Bacillus subtilis* which lack dipicolinic acid. J Bacteriol **182:**5505-5512.

27. **Setlow B, Cowan AE, Setlow P.** 2003. Germination of spores of *Bacillus subtilis* with dodecylamine. J Appl Microbiol **95:**637-648.

28. **Yi X, Setlow P.** 2010. Studies of the commitment step in the germination of spores of *Bacillus* species. J Bacteriol **192:**3424-3433.

29. **Yi X, Bond C, Sarker MR, Setlow P.** 2011. Efficient inhibition of germination of coat-deficient bacterial spores by multivalent metal cations, including terbium (Tb^{3+}). Appl Environ Microbiol **77:**5536-5539.

30. **Burg TP, Godin M, Knudsen SM, Shen W, Carlson G, Foster JS, Babcock K, Manalis SR.** 2007. Weighing of biomolecules, single cells and single nanoparticles in fluid. Nature **446:**1066-1069.

31. **Feijó Delgado F, Cermak N, Hecht VC, Son S, Li Y, Knudsen SM, Olcum S, Higgins JM, Chen J, Grover WH, Manalis SR.** 2013. Intracellular water exchange for measuring the dry mass, water mass and changes in chemical composition of living cells. PLoS One **8:**e67590.

32. **Lee J, Shen W, Payer K, Burg TP, Manalis SR.** 2010. Toward attogram mass measurements in solution with suspended nanochannel resonators. Nano Lett **10:**2537-2542.

33. **Tisa LS, Koshikawa T, Gerhardt P.** 1982. Wet and dry bacterial spore densities determined by buoyant sedimentation. Appl Environ Microbiol **43:**1307-1310.

34. **Grover WH, Bryan AK, Diez-Silva M, Suresh S, Higgins JM, Manalis SR.** 2011. Measuring single-cell density. Proc Natl Acad Sci U S A **108:**10992-10996.

35. **Carrera M, Zandomeni RO, Fitzgibbon J, Sagripanti JL.** 2007. Difference between the spore sizes of *Bacillus anthracis* and other *Bacillus* species. J Appl Microbiol.

102:303-312.

36. **Carrera M, Zandomeni RO, Sagripanti JL.** 2008. Wet and dry density of *Bacillus anthracis* and other *Bacillus* species. J Appl Microbiol **105:**68-77.

37. **Ghosal S, Leighton TJ, Wheeler KE, Hutcheon ID, Weber PK.** 2010. Spatially resolved characterization of water and ion incorporation in *Bacillus* spores. Appl Environ Microbiol **76:**3275-3282.

38. **Plomp M, Carroll AM, Setlow P, Malkin AJ.** 2014. Architecture and assembly of the *Bacillus subtilis* spore coat. PLoS One **9:**e108560.

39. **Eichenberger P, Fujita M, Jensen ST, Conlon EM, Rudner DZ, Wang ST, Ferguson C, Haga K, Sato T, Liu JS, Losick R.** 2004. The program of gene transcription for a single differentiating cell type during sporulation in *Bacillus subtilis*. PLoS Biol **2:**e328.

40. **Setlow P.** 2013. Summer meeting 2013--when the sleepers wake: the germination of spores of *Bacillus* species. J Appl Microbiol **115:**1251-1268.

41. **Velásquez J, Schuurman-Wolters G, Birkner JP, Abee T, Poolman B.** 2014. *Bacillus subtilis* spore protein SpoVAC functions as a mechanosensitive channel. Mol Microbiol **92:**813-823.

42. **Imamura D, Kuwana R, Takamatsu H, Watabe K.** 2011. Proteins involved in formation of the outermost layer of *Bacillus subtilis* spores. J Bacteriol **193:**4075-4080.

43. **He LM, Tebo BM.** 1998. Surface charge properties of and Cu(II) adsorption by spores of the marine *Bacillus* sp. strain SG-1. Appl Environ Microbiol **64:**1123-1129.

44. **Chen X, Mahadevan L, Driks A, Sahin O.** 2014. Bacillus spores as building blocks for stimuli-responsive materials and nanogenerators. Nat Nanotechnol **9:**137-141.

624 45. **McKenney PT, Driks A, Eichenberger P.** 2013. The *Bacillus subtilis* endospore:
625 assembly and functions of the multilayered coat. Nat Rev Microbiol **11**:33-44.
626 46. **Popham DL, Gilmore ME, Setlow P.** 1999. Roles of low-molecular-weight penicillin-
627 binding proteins in *Bacillus subtilis* spore peptidoglycan synthesis and spore properties. J
628 Bacteriol **181:**126-132.
629 47. **Meador-Parton J, Popham DL.** 2000. Structural analysis of *Bacillus subtilis* spore
630 peptidoglycan during sporulation. J Bacteriol **182:**4491-4499.
631

Table 1*

Strain	Genotype
PS533	wild-type
PS3328 (Tc^r)	*cotE*
PS3634	*cotXYZ*
PS3735	*spoVID*
PS3736	*cotH*
PS3740 (Cm^r)	*cotE*
PS3738 (Tc^r)	*safA*
PS4133	*cotB*
PS4134	*cotO*
PS4149 (Sp^r)	*gerE*
PS4150 (Tc^r Sp^r)	*cotE gerE*
PS4427 (Cm^r Tc^r)	*cotE safA*

*Sources of all strains are given in references 24 and 38 or generated in this work as described in Methods. Abbreviations used are resistance to: Cm^r-chloramphenicol (5 μg/ml); Tc^r – tetracycline 10 μg/ml; and Sp^r – spectinomycin 100 μg/ml.

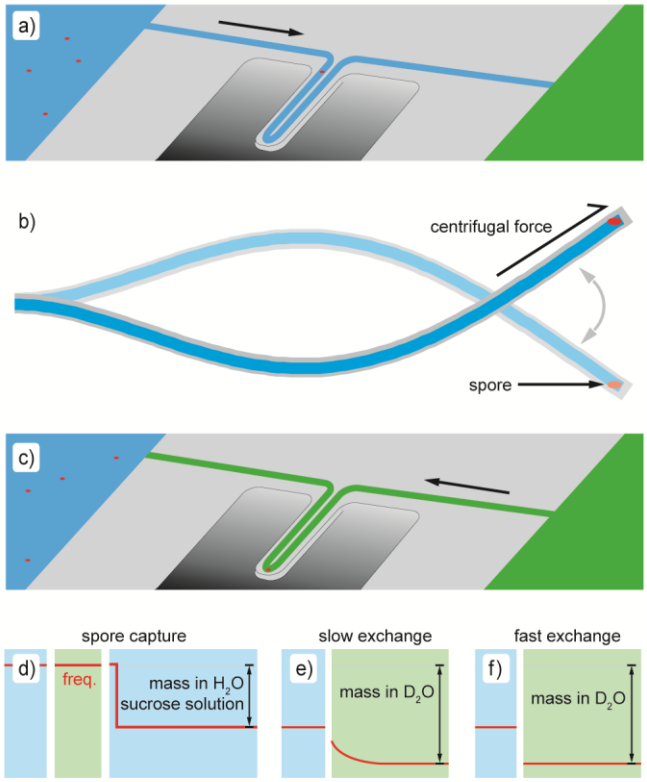

Fig. 1. Measurement schematic. The buoyant mass of individual spores is determined as they pass through a fluid channel embedded in a resonating cantilever (a). Spores can also be trapped at the end of the cantilever (b; cross section) by centrifugal force. The fluid within the resonator can be exchanged with the fluid in the other bypass (c), while the spore remains trapped. The expected mass signal is demonstrated for spore capture (d) and for slow (e) and fast (f) H_2O to D_2O exchange.

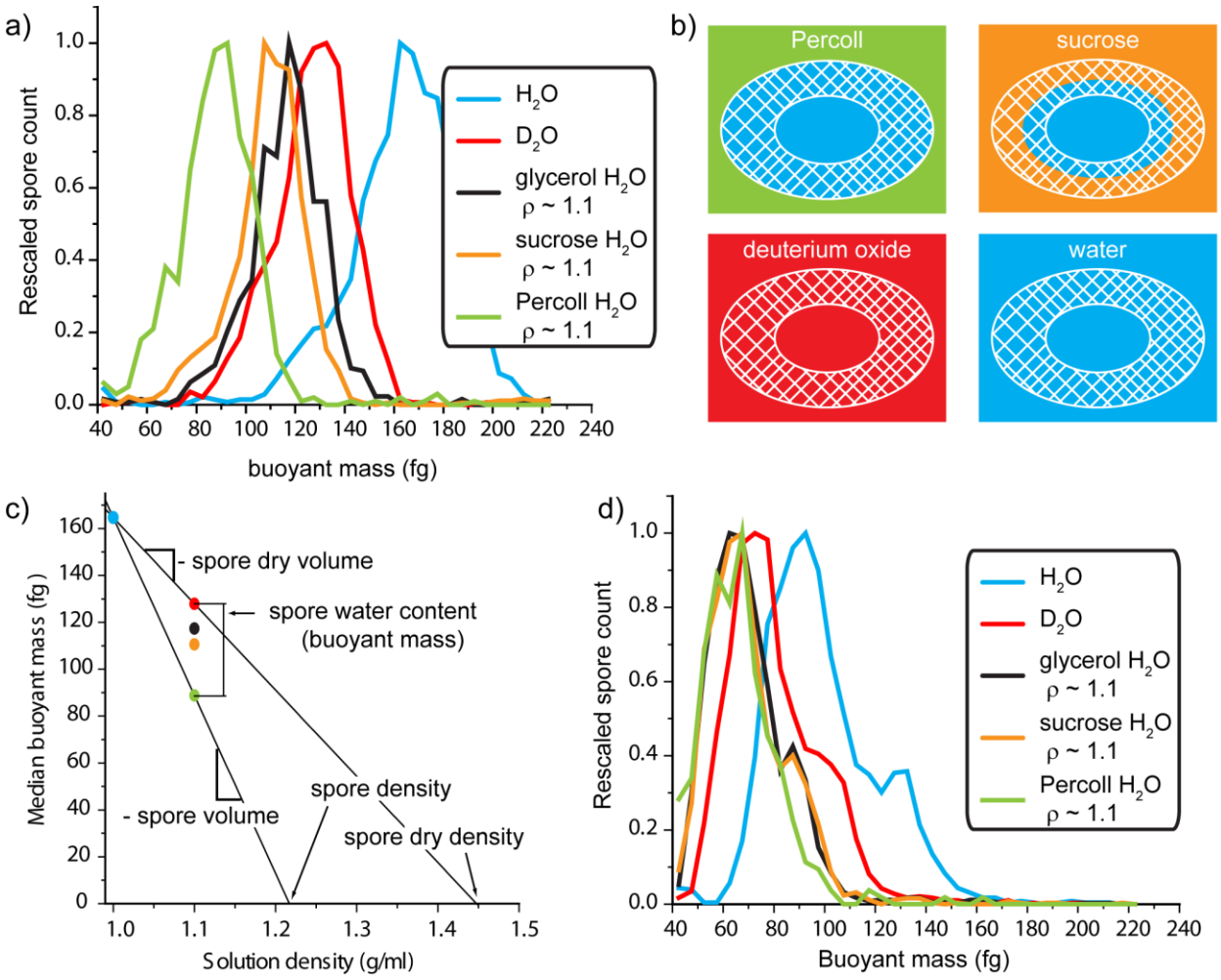

Fig. 2. The buoyant mass distributions for individual wild-type spores are shown (a) in various solutions. These molecules permeate the spores to different extents (b) and the resulting differences in buoyant mass can be used to calculate a number of biophysical parameters for the spores (c). The buoyant mass profiles of PS4150 (*cotE gerE*) (d) spores are shown in the same solutions.

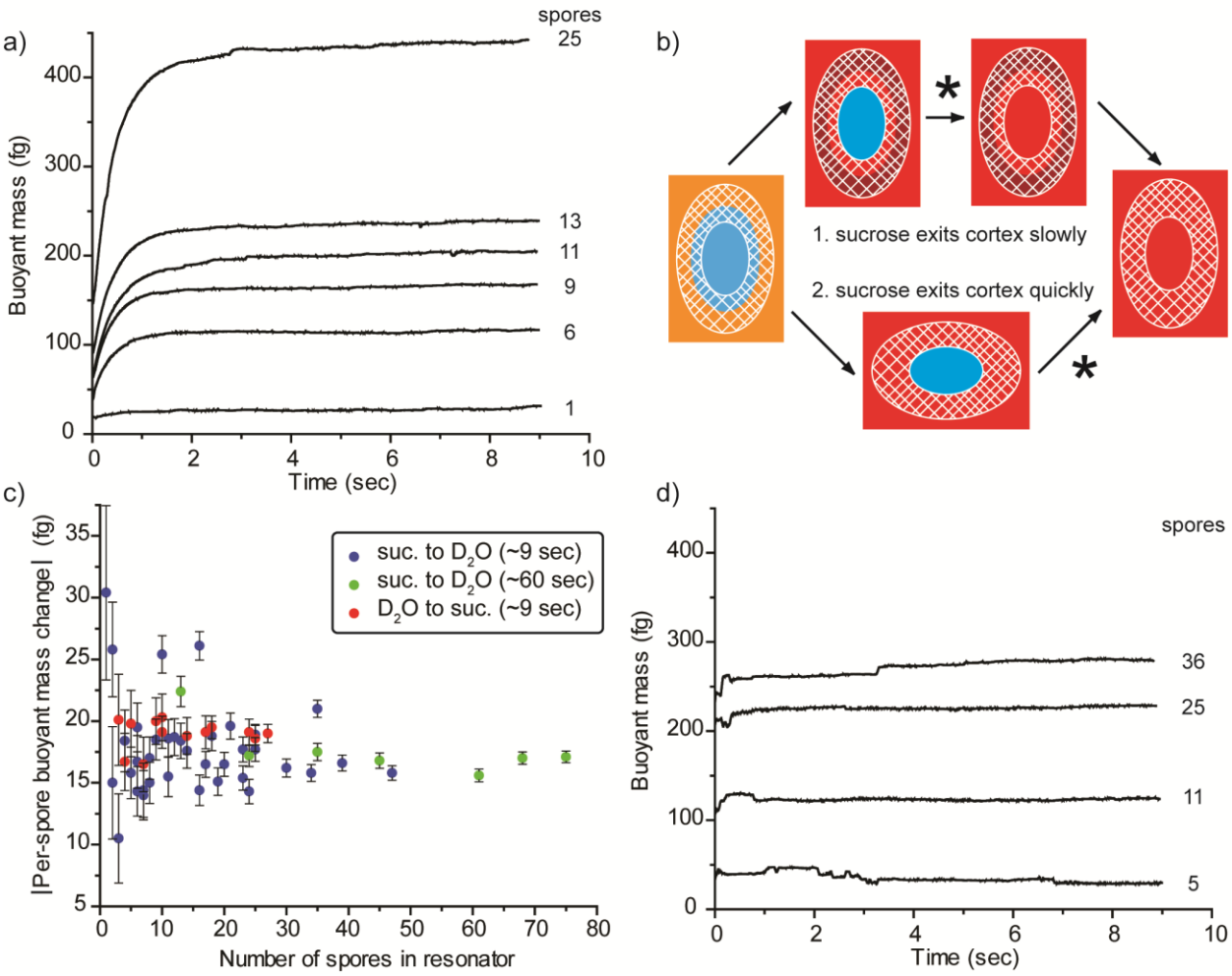

665

666 Fig. 3. The buoyant mass of spores 'trapped' at the tip of the cantilever is observed immediately
667 after the resonator is exchanged from an H_2O-sucrose (25%) solution to pure D_2O. Wild-type
668 spores (a) show a slow increase in buoyant mass from the replacement of internal H_2O with D_2O.
669 Sucrose leaving the spore is noted with an asterisk in alternate scenarios (b) where it occurs
670 either after replacement of internal H_2O with D_2O or before this exchange occurs. These
671 scenarios can be evaluated by quantifying the total change in buoyant mass per spore for
672 reactions that occur over different time scales and in the reverse order as shown in (c). For
673 example, data from (a) and replicate experiments are shown in blue. The experimental variation
674 observed here is greater than the calculated error bars because spores do not remain in exactly

675 the same position as the direction of fluid flow is switched back and forth and the SMR's
676 frequency is highly dependent on the position of mass within the resonator. Similarly,
677 irregularities are seen in the kinetic traces of some experiments as spores shift position. The
678 buoyant mass change for *cotE gerE* spores (d) takes place on a timescale that less than the
679 temporal resolution of the measurement.

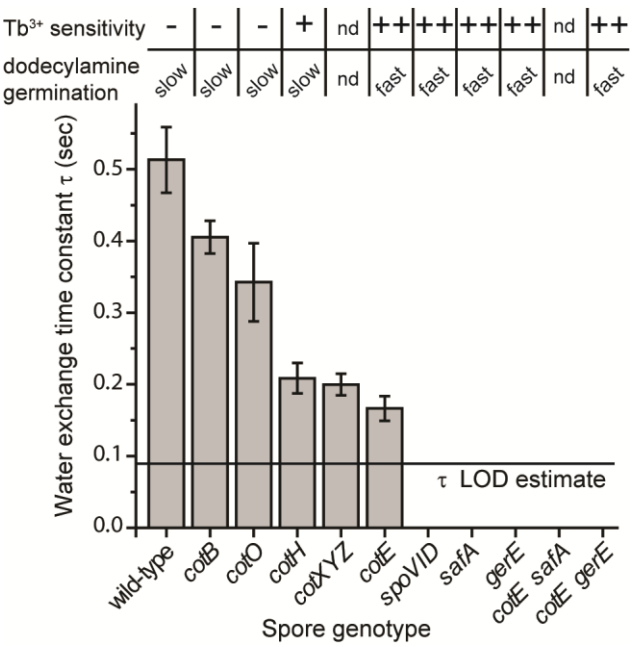

Fig. 4. The time constants for H_2O to D_2O exchange are determined by fitting the kinetic traces in Fig. 3a,d and S2 to an exponential decay equation, $y=a+b(1-e^{-t/\tau})$. Under the flow conditions used for these experiments, it takes ~200 msec to completely replace the fluid in the embedded channel. Time constants were not determined for spores in which the exchange appears to be complete by this time. Rather, we estimate an upper bound as our limit of detection (LOD), here assumed to be 0.09 sec (yielding an exchange that is 90% complete after 200 msec), indicated by a horizontal line on the plot above. The Tb^{3+} sensitivity of L-valine germination ((-) indicates minimal inhibition, (+) indicates intermediate inhibition, and (++) indicates nearly complete inhibition, and rates of dodecylamine germination (slow germination is <50% of the rate of fast germination) are taken from Fig. 5, and data not shown.

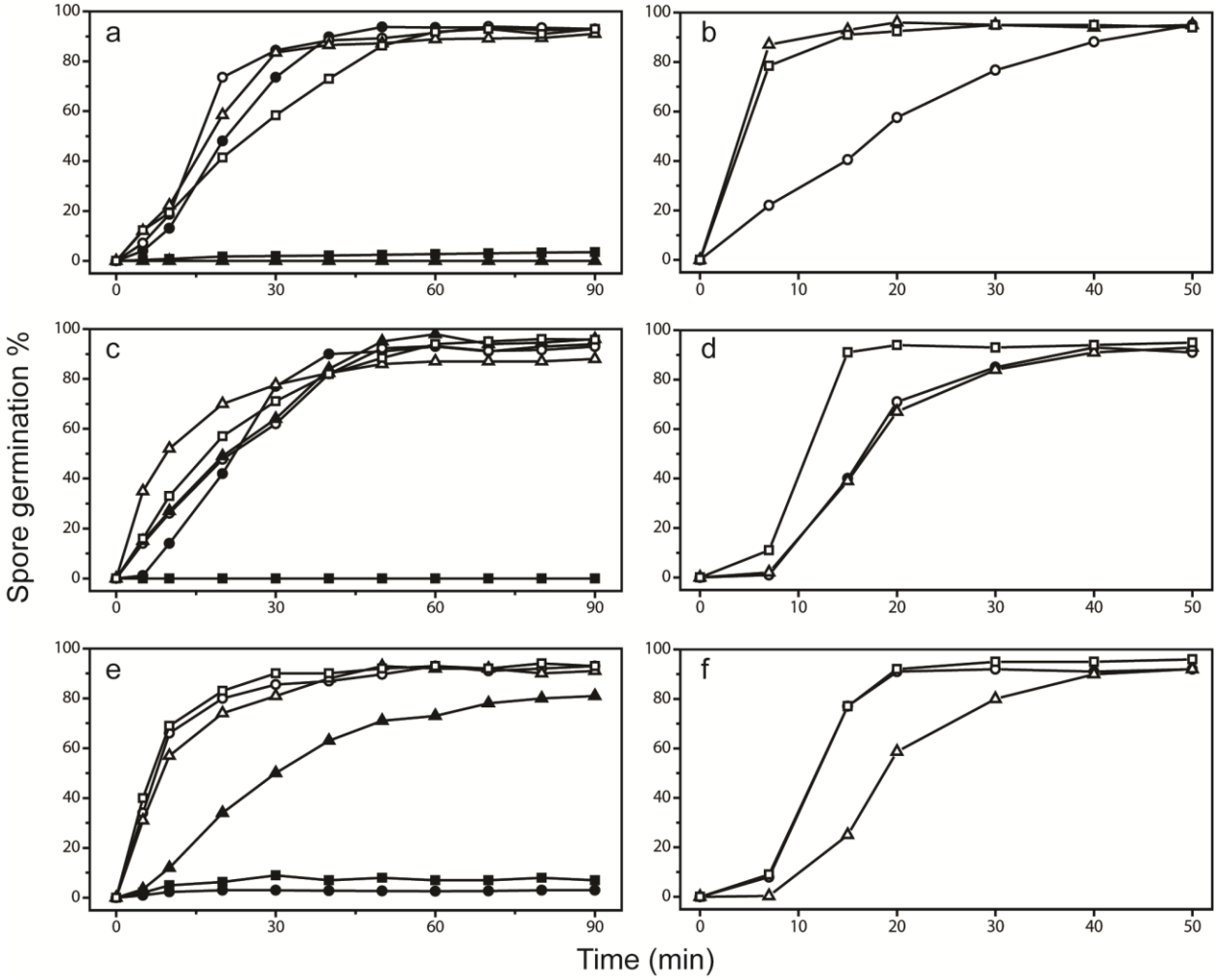

Fig. 5a-f. L-Valine and dodecylamine germination of spores of wild-type and coat mutant *B. subtilis* spores. Spores of various strains were germinated with either (a,c,e) L-valine or (b,d,f) dodecylamine with $TbCl_3$ present either from the beginning of germination (●,▲,■) or added at various times (○,△,□) as described in Methods. The symbols denoting the spores analyzed in the various panels are: a,b) ○,● - PS533 (wt), △,▲ - PS4150 (*cotE gerE*); and □,■ - PS3328 (*cotE*); c,d) ○,● - PS4133 (*cotB*); △,▲ - PS4134 (*cotO*); and □,■ - PS4149 (*gerE*); and e,f) ○,● - PS3735 (*spoVID*); △,▲ - PS3736 (*cotH*); and □,■ - PS3738 (*safA*).